Bioconvection

Hefei Hu

December 11, 2007

Abstract

Bioconvection patterns, which are a collective phenomenon, usually appear due to upswimming of micro-organisms that are a little denser than water in suspensions. When the upper surface of the suspensions becomes too dense due to the gathering of micro-organisms, it becomes unstable and micro-organisms fall down to cause bioconvection. This essay will review the theoretical models and simulations, as well as experiments of bioconvection patterns.

1. Introduction

Bioconvection occurs because micro-organisms, which are denser than water, swim upwardly on average. When the upper surface of the suspensions is too dense due to the gathering of micro-organisms, it becomes unstable and micro-organisms fall down to cause bioconvection. Return upswimming micro-organisms maintain this bioconvection pattern.

There are two typical types of upswimming micro-organisms that are usually used in bioconvection experiments: bottom-heavy alga and certain oxytactic bacteria. Although the bioconvection patterns formed by them are very similar, the mechanisms of orientation are different (Hill and Pedley, 2005).

Bottom-heavy micro-organisms swim upward in still water because of the asymmetric mass distribution. When such micro-organisms are in a flow field, the swimming direction is determined by the balance between the toques due to viscous drag arising from shear flow and gravity acting on the cell (Pedley *et al*., 1988). Cells tend to swim towards regions of downwelling fluid, which is known as gyrotaxis. The bioconvection experiments by using oxytactic bacteria are performed in a chamber with the upper level of suspensions open. These bacteria consume oxygen and swim up gradients of oxygen.

Theoretical models are established for both bottem-heavy alga and oxytactic bacteria. Numerical simulations of bioconvection are also carried out.

2. Models

2.1 Continuum models

Continuum models are proposed on the assumption that the cell-cell interaction is neglected and the length scale of the chamber as well as the distribution of concentration are large compared with the cell dimension, so that variables are considered to be continuous (Pedley et al., 1988; Pedley and Kessler, 1990; Hill and Pedley, 2005). The suspension is considered to be dilute, so that the volume concentration $nv \ll 1$, where $n(x,t)$ is the number density of cells and v is the average volume of a cell. $u(x,t)$ is defined as the bulk velocity. Assuming water and cells cannot be compressed, followed by volume conservation, we have

$$\nabla \cdot \vec{u} = 0 \qquad (2.1)$$

The conservation of momentum and cell number gives

$$\rho \frac{D\vec{u}}{Dt} = -\nabla p_e + nv\Delta\rho\vec{g} + \nabla \cdot \vec{\Sigma} \qquad (2.2)$$

$$\frac{\partial n}{\partial t} = -\nabla \cdot [n(\vec{u} + \vec{V_c}) - D \cdot \nabla n] \tag{2.3}$$

Here, $D\vec{u}/Dt \equiv \partial\vec{u}/\partial t + (\vec{u} \cdot \nabla)\vec{u}$, $p_e(x,t)$ is the pressure excess over hydrostatic, $\Delta\rho$ is the density difference between cells and water, g is the gravity constant, $\vec{\Sigma}(x,t)$ is the deviatoric stress tensor, $\vec{V_c}$ is the mean cell swimming velocity and $D(x,t)$ is the cell diffusivity tensor.

For bottom-heavy micro-organism, $\vec{V_c} = V_s\langle\hat{p}\rangle$, where $\hat{p}$ is the unit direction vector and $\langle\ \rangle$ represents the ensemble average defined by $\int(\cdots)f(\hat{p})d^2\hat{p}$. Here $f(p)$ is the density function of probability which should satisfy the Fokker-Planck equation

$$\frac{\partial f}{\partial t} + \nabla_p \cdot (\dot{\hat{p}}f) = D_r\nabla_p^2 f \tag{2.4}$$

The cell diffusivity tensor D is defined by

$$\vec{D}(t) = \int_0^\infty \langle\vec{V_r}(t)\vec{V_r}(t-t')\rangle, \tag{2.5}$$

Where $\vec{V_r} = \vec{V_s}\hat{p} - \vec{V_c}$.

If V_s is a constant, D is approximated as

$$D = V_s^2\tau\langle(\hat{p}-\langle\hat{p}\rangle)(\hat{p}-\langle\hat{p}\rangle)\rangle, \tag{2.6}$$

where τ is the direction correlation time

Also, Σ is assumed as

$$\Sigma = 2\mu E, \tag{2.7}$$

where μ is the fluid viscosity and E is the bulk rate of strain tensor.

In the infinite environment, even though cells are swimming upwards, the concentration of cells $n_0(x,t)$ does not change. A linear stability theory was applied to investigate in stability, and small perturbation amplitude ε is introduced to the variables which can be expressed as

$$n = n_0 + \varepsilon n', \quad u = \varepsilon u', \quad p_e = p_{e0} + \varepsilon p_e', \quad p = k + \varepsilon p', \tag{2.8}$$

Substituting (2.8) into the governing equations (2.1), (2.2), (2.3) and (2.4), and keeping only linear terms give linear differential equations with constant coefficients. Then the instability can be examined in terms of Fourier modes. For the suspension of finite depth, instability occurs only if the gyrotactic Rayleigh number R exceeds a critical value. R is defined as

$$R = \rho V_s^2 B / \mu ,\qquad(2.9)$$

where B is the gyrotactic orientation parameter

The Nonlinear analysis of deep gyrotactic Bioconvection was explored by Bees and Hill (Bees and Hill, 1998). The distance between the very first plumes can be predicted by analyzing the accumulative behaviour of individual micro-organisms. On the assumption of no vertical variation, steady state and traveling solutions are found.

For oxytactic bacteria, the governing equations are still applied, but the mean cell swimming velocity was assumed as

$$V_c = \chi \nabla C ,\qquad(2.10)$$

Where χ is a constant and C is oxygen concentration that satisfies equation

$$\frac{DC}{Dt} = D_c \nabla^2 C - kn ,\qquad(2.11)$$

where Dc is the oxygen diffusivity.

2.2 Microscale models

In 1995, Dillon *et al*. established a microscale model of bacterial swimming (Dillon *et al*., 1995), which represents micro-organisms as individual microbes. In this model, very detailed geometry, such as flagellar rotation, hydrodynamic interaction of swimming microbes and microbial uptake, are considered. Dillon *et al*. also performed the simulations of this model, but only several microbes were described in the simulation due to the detailed geometry considered in this model. Some of prelim simulation results are presented in the next section.

2.3 Particle models

A particle model of chemotaxis was proposed by Hopkins and Fauci (Hopkins and Fauci, 2002). They described micro-organisms as individual particles and ignored the geometry (like flagellar action) in detail. By using this simplified description of micro-organisms, they managed to perform simulations with a large number of particles. The assumption of homogeneous and incompressible dilute fluids was also made. N discrete micro-organisms located at x_k, $k = 1, 2, \ldots, N$ are considered in a rectangular region of fluid, so that the governing equations are obtain:

$$\rho \frac{D\vec{u}}{Dt} = -\nabla p + \mu \nabla^2 \vec{u} + \Delta \rho v \vec{g} \sum_{k=1}^{N} \delta(\vec{x} - \vec{x}_k) \,, \tag{2.12}$$

$$\nabla \cdot \vec{u} = 0 \,, \tag{2.13}$$

$$\frac{\partial c}{\partial t} + \vec{u} \cdot \nabla c = D \nabla^2 c - R(c) \sum_{k=1}^{N} \delta(\vec{x} - \vec{x}_k) \,, \tag{2.14}$$

$$\frac{dx_k}{dt} = \vec{u}(x_k, t) + s_k \vec{p}_k \,, \quad k = 1, 2, ..., N \,, \tag{2.15}$$

where $c(x,t)$ is the chemical concentration and $R(c)$ is the consumption rate which is dependent on the local concentration.

3. Numerical simulations

Ghorai and Hill have been carrying out numerical simulations of gyrotactic bioconvection for several years (Ghorai and Hill, 1999, 2000, 2007). They used continuum models of Pedley *et al*. (Pedley and Hill, 1988) and solved the governing equations numerically to investigate the existence and stability of periodic arrays of two-dimensional gyrotactic plumes in bioconvection (Ghorai and Hill, 2000). Some parameters, such as suspension depth, cell concentration, etc., are varied to examine the dependence of the wavelengths on the depth of these parameters. The simulations demonstrate that wavelengths slightly increase with the depth of suspensions, not quite consistent with the experiment (Bees and Hill, 1997). This inconsistence occurs probably because the simulations describe 2D system, but the experiments are performed in three dimensions. The simulations also show wavelengths decrease with an increase of concentration, consistent with experiments. The numerical simulations for different suspension depth are shown in the following figures (duplicated from Ghorai and Hill, 2000). Fig.1 and fig.2 show the evolution of cells in the chamber with same widths, but with different depths. Fig. 3 shows the comparison of convection patterns at certain time for the different depths. In 2007, Ghorai and Hill managed to simulate gyrotactic bioconvection in three dimensions. Fig. 4 shows the evolution of a single plume in three dimensions.

Dillon *et al.* simulated micro-organism swimming by using microscale models (Dillon et al., 1995). The simulations showed there is strong local hydrodynamics interaction between cells via the fluid media. Fig. 5 shows the swimming of eight chemotactic cells with hydrodynamics in the time sequence of frames. Two cells are marked. Fig. 6 shows the cells trajectories in a rum and tumble model.

Matthew *et al*. used particle models to performe simulations of bioconvection parttern. Fig. 7 shows one example of parttern time evolution, consisting of approximately

85,7000 particles.　From those calculations, they demonstrated plume stability decrease with depth, and plume wavelengths increase with depth.
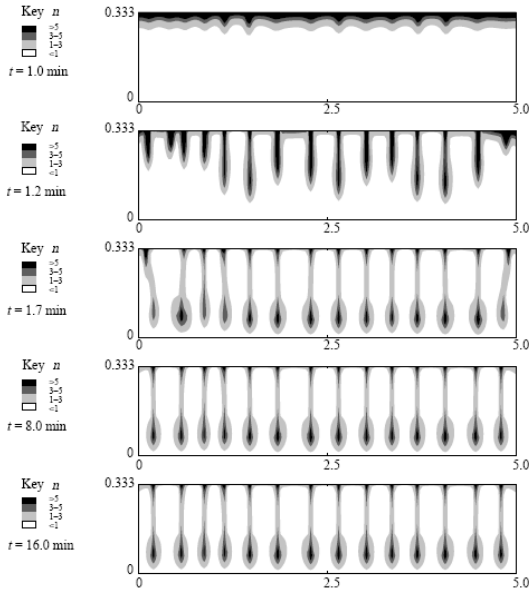

Fig. 1 Concentration of cells at different time in 0.333 cm deep and 5 cm wide chamber
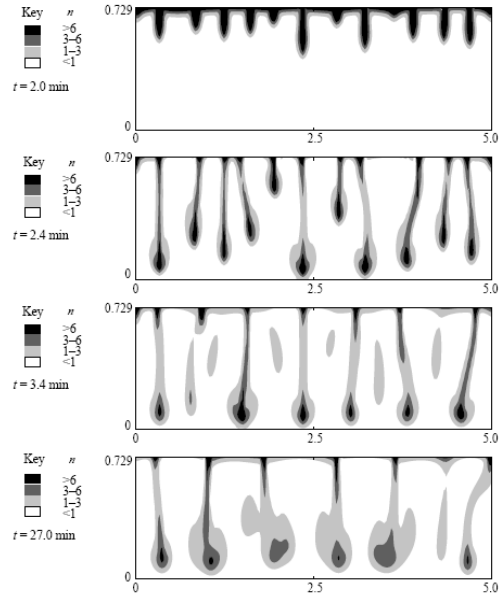

Fig. 2 Concentration of cells at different time in 0.729 cm deep and 5 cm wide chamber
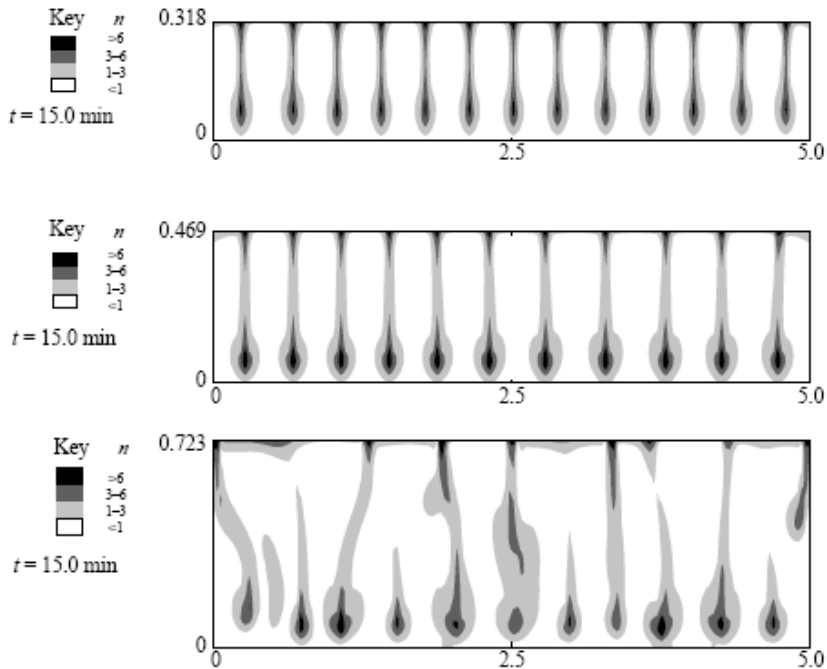

Fig. 3 Concentration of cells at certain time in chambers of 5 cm width but of different depths
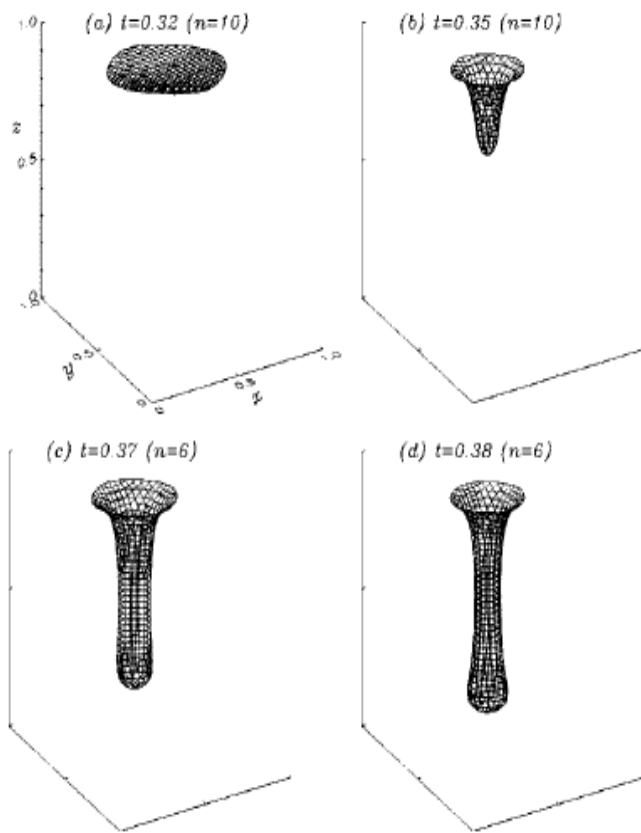
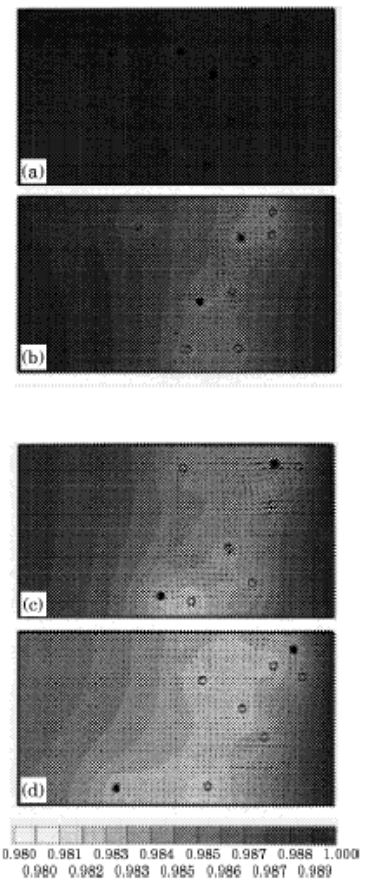Fig. 4 Pattern formation of a single gyrotactic plume in three dimensions

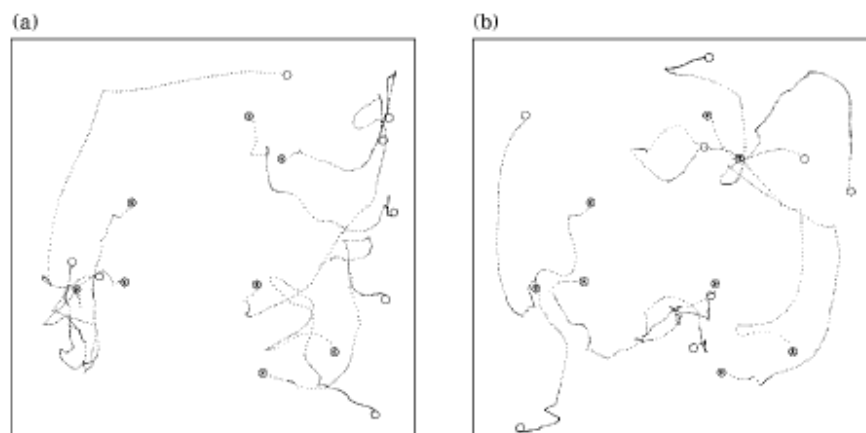Fig. 5 Swimming of eight chemotactic cells with hydrodynamics in the time sequence of frames

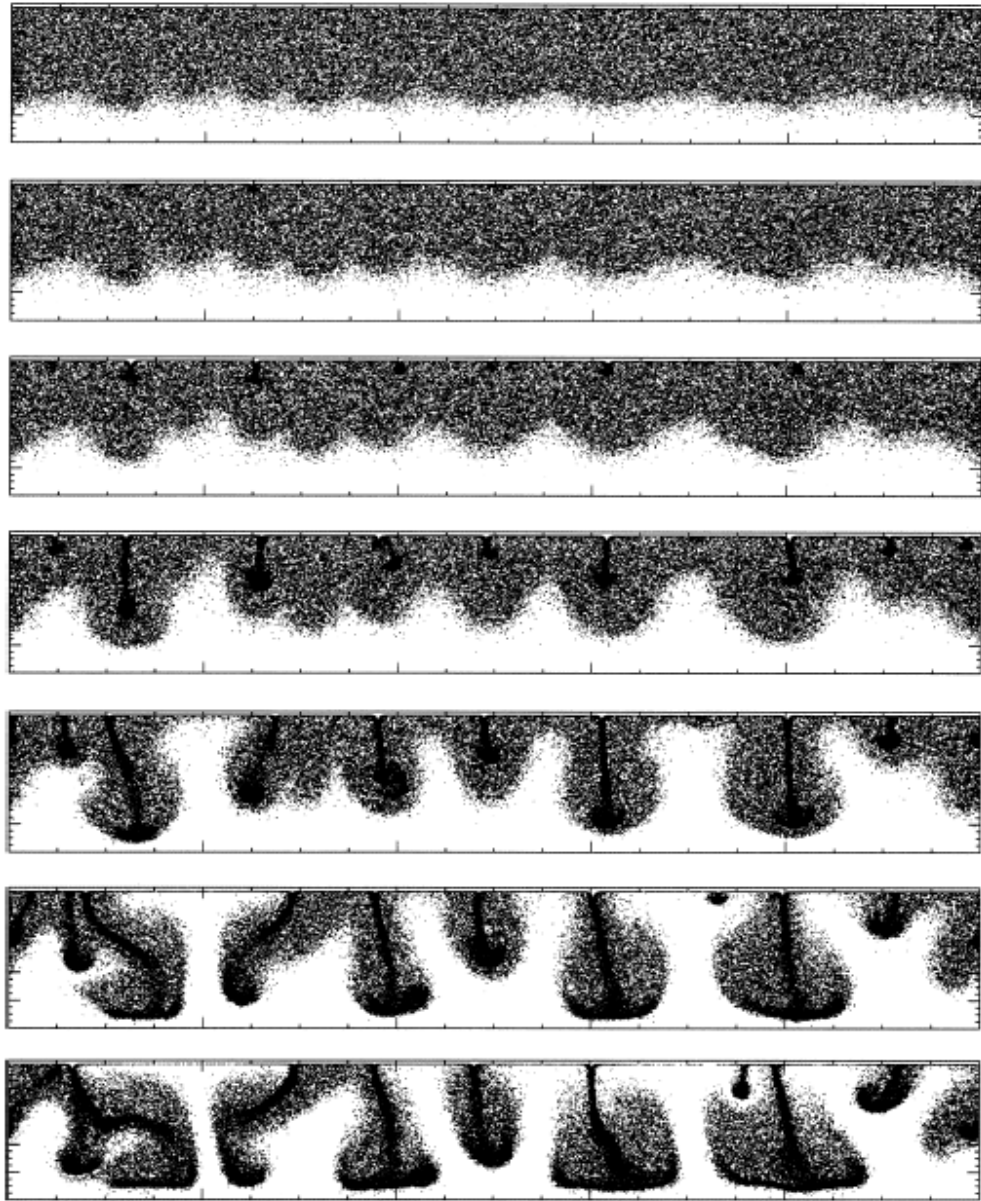Fig. 6 cells trajectories in a rum and tumble model

Fig. 7 Time evolution of convection patterns in particle models, consisting of approximately 85,7000 particles

4. Experiments

Bioconvection patterns have been known since 1848, and many observations were reported since then. Fig. 8 shows a series of snapshots of a suspension of the aerobic bacteria B. subtilis (Kessler et al., 1995). The suspension is initially uniform. When more and more *B. subtilis* aggregate at the surface of the suspension, instability occurs, and plumes appear.

Fig. 8 a series of snapshots of a suspension of the aerobic bacteria B. subtilis

Bees and Hill carried out controlled experiments and gave quantitatively analysis on bioconvection patterns formed by suspensions of the single-celled alga *Chlamydomonas nivalis* (Bees and Hill, 1997). The formation of the bioconvection patterns were captured by a video camera every 10 second. For each of the measurements, 9 images were recorded. Then two-dimensional Fourier transforms were used to calculate the wavelengths of the bioconvection patterns, and to determine the dominant unstable wavenumber, "which is defined as the number of complete sinusoidal waves in a length of the same size as the image's width", as a function of time, cell concentration and suspension depth. The results are presented in Table 1.

Expt no.	Cell concentration (cm^{-3})	Suspension depth (cm)	k_0 per dish	k_∞ per dish	λ_0 (cm)	λ_∞ (cm)	Notes
1	2.75×10^6	0.333	14.09	NA	0.369	NA	
2	2.07×10^6	0.396	10.71	NA	0.486	NA	
3	6.31×10^6	0.365	19.47	22.57	0.267	0.230	
4	3.06×10^6	0.444	11.10	17.30	0.468	0.301	
5	0.808×10^6	0.522	10.80	NA	0.481	NA	Mixed modes
6	1.02×10^6	0.729	7.50	NA	0.693	NA	Mixed modes
7	0.886×10^6	0.399	12.48	NA	0.417	NA	Mixed modes
8	1.64×10^6	0.381	15.76	NA	0.330	NA	Slow to develop
9	2.30×10^6	0.456	15.10	NA	0.344	NA	Slow to develop
10	1.88×10^6	0.690	10.00	NA	0.520	NA	Slow to develop
11	2.81×10^6	0.282	15.40	NA	0.338	NA	Mixed modes
12	2.47×10^6	0.528	8.87	19.10	0.586	0.272	Two mixed modes, starts in centre
13	2.15×10^6	0.645	10.08	18.61	0.516	0.279	Mixed modes, starts in centre
14	1.89×10^6	0.384	14.96	16.73	0.348	0.311	Images recorded every 30 s
15	1.89×10^6	0.318	14.20	10.64	0.366	0.489	Images recorded every 20 s
16	3.62×10^6	0.310	17.15	14.54	0.303	0.358	
17	1.89×10^6	0.469	7.34	17.18	0.708	0.303	Two peaks, left dominant
18	1.89×10^6	0.469	14.70	14.79	0.354	0.352	Two peaks, left dominant
19	1.89×10^6	0.469	8.63	15.62	0.603	0.333	Two peaks, right dominant
20	1.89×10^6	0.723	9.97	15.11	0.522	0.344	
21	1.89×10^6	0.384	15.12	15.67	0.344	0.332	
22	2.09×10^6	0.355	14.25	16.66	0.365	0.312	
23	4.19×10^6	0.468	13.87	22.20	0.375	0.234	
24	4.19×10^6	0.291	17.26	20.62	0.301	0.252	
25	4.19×10^6	0.186	27.67	17.48	0.188	0.297	
26	4.30×10^6	0.282	19.66	22.52	0.264	0.231	
27	4.30×10^6	0.282	17.76	21.89	0.293	0.238	
28	4.30×10^6	0.282	15.75	24.19	0.330	0.215	
29	4.30×10^6	0.282	17.45	23.52	0.298	0.221	Images recorded every 20 s
30	11.8×10^6	0.342	18.08	36.84	0.288	0.141	
31	4.00×10^6	0.297	16.71	28.03	0.311	0.186	
32	15.0×10^6	0.195	28.24	28.02	0.184	0.186	
33	11.8×10^6	0.118	34.84	32.95	0.149	0.158	
34	11.8×10^6	0.168	30.59	32.72	0.170	0.159	
35	3.60×10^6	0.324	15.71	17.30	0.331	0.301	
36	11.8×10^6	0.342	15.70	25.58	0.331	0.203	
37	4.30×10^6	0.228	23.09	34.15	0.225	0.152	
38	12.2×10^6	0.300	28.73	45.19	0.181	0.115	
39	12.2×10^6	0.300	29.86	43.05	0.174	0.121	Images recorded every 30 s

Table 1.   The results of 39 measuremnts. λ is the physical wavelength, defined as $\lambda = I_w/k$, where k is the wavelength.   The subscript 0 means the first unstable mode and infinity means the final mode.

5. Conclusion

Several models were established for bioconvection.   Computational simulations in different models were also performed, which gave the theoretical prediction of bioconvection pattern formation, and were consistent with or very close to experimental observations.   However, most models are only valid on the assumption of dilute suspensions, so that the models of concentrated suspensions would be further investigated.

References

Bees, M.A. and Hill, N. A., **1997** Wavelengths of bioconvection patterns, *J. Exp. Bio.*, 200, 1515–1526
.

Bees, M.A. and Hill, N.A., **1998**, Linear bioconvection in a suspension of randomly-swimming, gyrotactic micro-organisms. *Phys.Fluids* 10, 1864–1881.

Dillon, R., Fauci, L. and Gaver, D. **1995,** A microscale model of bacterial swimming, chemotaxis and substrate transport. *J. Theor. Biol.* 177, 325-340.

Ghorai, S., Hill, N.A., **1999**. Development and stability of gyrotactic plumes in bioconvection. *J. Fluid Mech.* 400, 1–31.

Ghorai, S., Hill, N.A., **2000**. Wavelengths of gyrotactic plumes in bioconvection. *Bull. Math. Biol.* 62, 429–450.

Ghorai, S., Hill, N.A., **2007**, Gyrotactic bioconvection in three dimensions. *Phys. Fluid*. 19, 054107

Hillesdon, A.J., Pedley, T.J., **1996**. Bioconvection in suspensions of oxytactic bacteria: linear theory. *J. Fluid Mech.* 324, 223–259

Hill, N.A. and Pedley, T.J., **2005** Bioconvection. *Fluid Dynamics Research*, 37,1-20.

Hopkins, M. M. and Fauci, L. J. , **2002**, A computational model of the collective fluid dynamics of motile micro-organisms, *J. Fluid Mech*. 455, 149-174.

Kessler, J. O., Strittmatter, R. P., Swartz, D. L. and others **1995** Paths and patterns: The biology and physics of swimming bacterial populations. In Biological Fluid Dynamics (ed.C. P. Ellington and T. J. Pedley), vol. 49, Symp. Soc. Expl Biol, pp. 91

Pedley, T.J., Hill, N.A., Kessler, J.O., **1988**. The growth of bioconvection patterns in a uniform suspension of gyrotactic microorganisms. *J. Fluid Mech*. 195, 223–238.

Pedley, T.J., Kessler, J.O., **1990**. Ane w continuum model for suspensions of swimming micro-organisms. *J. Fluid Mech.* 212, 155–182.